Inorganic Chemistry

Forum Article

pubs.acs.org/IC

Role of Metal Ions in the Self-assembly of the Alzheimer's Amyloid-β Peptide

Peter Faller,* Christelle Hureau, and Olivia Berthoumieu

CNRS, LCC (Laboratoire de Chimie de Coordination), 205 route de Narbonne, BP 44099, F-31077 Toulouse Cedex 4, France
Université de Toulouse, UPS, INPT, F-31077 Toulouse Cedex 4, France

ABSTRACT: Aggregation of amyloid-β (Aβ) by self-assembly into oligomers or amyloids is a central event in Alzheimer's disease. Coordination of transition-metal ions, mainly copper and zinc, to Aβ occurs in vivo and modulates the aggregation process. A survey of the impact of Cu^{II} and Zn^{II} on the aggregation of Aβ reveals some general trends: (i) Zn^{II} and Cu^{II} at high micromolar concentrations and/or in a large superstoichiometric ratio compared to Aβ have a tendency to promote amorphous aggregations (precipitation) over the ordered formation of fibrillar amyloids by self-assembly; (ii) metal ions affect the kinetics of Aβ aggregations, with the most significant impact on the nucleation phase; (iii) the impact is metal-specific; (iv) Cu^{II} and Zn^{II} affect the concentrations and/or the types of aggregation intermediates formed; (v) the binding of metal ions changes both the structure and the charge of Aβ. The decrease in the overall charge at physiological pH increases the overall driving force for aggregation but may favor more precipitation over fibrillation, whereas the induced structural changes seem more relevant for the amyloid formation.

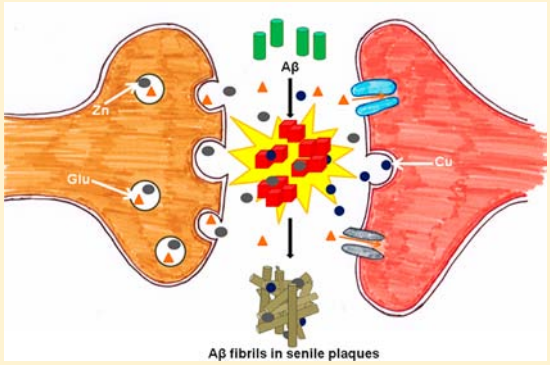

1. INTRODUCTION

1.1. Alzheimer's Disease (AD). AD is the most common cause of dementia in the elderly population. Symptoms of the disease are difficulty in remembering newly learned information (at the early stage), mood and behavior changes, memory loss, judgment alteration, and difficulties in daily and usual activities (www.alz.org/). Hence, the patients need constant attention from their caregivers. In addition, AD currently affects more than 30 million people worldwide. It is estimated that more than 100 million people will be affected by 2050, mainly because of the fast growth of the elderly population in developing countries (www.alz.co.uk).[1] AD socioeconomical impacts are thus very important, and the health-care system is under increasing pressure.

1.2. Amyloid-β. At a pathophysiological scale, AD is characterized by two hallmarks: extracellular senile plaques and intracellular neurofibrillary tangles (NFTs) of hyperphosphorylated τ protein. Amyloid plaques are mainly made of aggregated forms of a peptide, called amyloid-β (Aβ).[1] Aβ is a 39−43 residue polypeptide encompassing an N-terminal hydrophilic sequence and a C-terminal hydrophobic domain (Scheme 1).

According to the amyloid cascade hypothesis, senile plaques (also called amyloid plaques) and/or their precursors (smaller aggregates of Aβ) induce the formation of NFTs. This is in line with the fact that senile plaques can be detected before the observation of psychological and behavioral symptoms, placing the formation of plaques at an early stage of AD development.[1] However, healthy individuals can also have amyloid plaques, indicating that plaques are not the only factor in AD. Aβ is obtained by the cleavage of trans-membrane amyloid precursor protein (APP) by β- and γ-secretases. Aβ40, and to a lesser extent Aβ42, are the most abundant Aβ species produced in the brain and are present in the cerebrospinal fluid (CSF). While the Aβ40/Aβ42 ratio in the soluble fractions is approximately 1:9, Aβ42 is considered the most toxic peptide in line with a higher propensity to aggregate (Aβ40/Aβ42 ratio in plaques $\sim$ 1:2) and thus to initiate Aβ aggregation.[2,3]

1.3. Metal Ions ($Cu^{I/II}$, Zn^{II}, and $Fe^{II/III}$) in AD. Remarkably, high concentrations (in the millimolar range) of several transition-metal ions, mainly Cu^{II}, Zn^{II}, and Fe^{III}, are also found in these plaques,[4,5] with Cu^{II} and Zn^{II} being bound to the Aβ peptide.[6] In AD post-mortem brains, the amyloid plaques can be imaged by light microscopy using specific dyes, e.g., congo red and thioflavin T (ThT), two stains characteristic of β-sheet structure[7] (Table 1). Hence, because monomeric soluble Aβ is found in healthy persons, the path leading to the formation of Aβ aggregates is key for the etiology of the disease. Metal ions can also intervene in this process, via different routes, mainly by modulating Aβ aggregation.[8−12] Redox metal ions are also involved via reactive oxygen species (ROS) production,[13] and the two processes (Aβ aggregation and ROS production) can be linked together by oxidative damage on the Aβ peptide itself, leading to Aβ forms more prone to aggregation, such as, for instance, cross-linked dimeric species of Tyr10.[14]

Special Issue: Metals in Medicine and Health

Received: February 5, 2013
Published: April 22, 2013

   dx.doi.org/10.1021/ic4003059 | Inorg. Chem. 2013, 52, 12193−12206

Scheme 1. Amino Acid Sequence (1 Letter Code) of the Two Most Abundant Forms of Aβ, i.e., Aβ42 and Aβ40, as well as the Truncated Aβ28 and Aβ16[a]

Aβ42 (Aβ1-42): DAEFRHDSGY[10]EVHHQKLVFF[20]AEDVGSNKGA[30]IIGLMVGGVV[40]IA
Aβ40 (Aβ1-40): DAEFRHDSGY[10]EVHHQKLVFF[20]AEDVGSNKGA[30]IIGLMVGGVV[40]
Aβ28 (Aβ1-28): DAEFRHDSGY[10]EVHHQKLVFF[20]AEDVGSNK
Aβ16 (Aβ1-16): DAEFRHDSGY[10]EVHHQK

[a]The color represents the amino acids involved in metal binding, with red as the main binding amino acids.

Table 1. Some Techniques To Measure Aggregation[a]

techniques	information, uses	pros	limitations
ThT fluorescence; congo red (birefringence or absorption change)	used for measurement of amyloids; oligomers might also switch upon ThT fluorescence but to a much lower extent	easy and in situ	no well-defined interaction; might interfere with aggregation
turbidity	measure for aggregation, mainly dependent on the size (no distinction between precipitates and amyloids)	easy, in situ, no labeling or additive	does not distinguish between fibrils and amorphous aggregates
dynamic light scattering	measures the size of the aggregates (no distinction between precipitates and amyloids)	in situ, no labeling or additive	more difficult to detect small size aggregates
microscopy (AFM and TEM)	size and form at high resolution; (mature) fibrils are well detected.	no labeling resolution of single aggregate; AFM can be in situ	not quantitative; interaction with surface might interfere; TEM depends on staining
CD or FTIR	secondary structure, monomer unstructured, amyloid β-sheet	in situ	CD: light scattering can interfere FTIR: high concentration needed
PICUP cross-linking	assumed to freeze out oligomers	stable because of cross-linking	might initiate covalent dimers; need vicinity of potential substrate (Tyr, etc., in Aβ)

[a]For a more detailed discussion of the pros and cons, see ref 25.

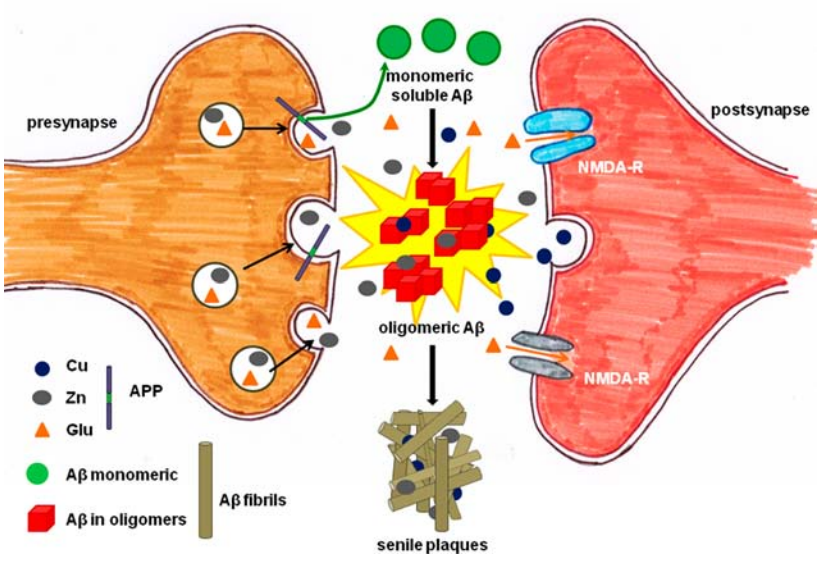

Figure 1. Scheme of the synaptic cleft where Aβ, Cu^{II}, and Zn^{II} can be found together in abnormally high concentration. Soluble monomeric Aβ peptides (green spheres) are obtained via the cleavage of APP protein, and $Cu^{I/II}$ and Zn^{II} are released by neuronal excitation and are involved in the Aβ aggregation process, leading to the formation of amyloid plaques detected in AD brains. Oligomeric intermediates are considered to be the most toxic species, inducing neuronal death.

As shown in Figure 1, Aβ aggregation takes place in the synaptic cleft where a high concentration of Zn^{II} (200−300 μM, compared with nanomolar to micromolar values for the concentration in the CSF)[15] can be transiently released upon neuronal excitation. Such Zn^{II}-rich neurons are a subclass of glutamatergic neurons and are found in the hippocampus, a key region for memory and one of the first struck in AD. The Zn^{II} released is not tightly bound to biological ligands and is thus considered as a labile pool, able to interact with weaker ligands. For $Cu^{I/II}$, the situation is less clear, but recent studies indicate that a similar labile $Cu^{I/II}$ pool (up to 10−100 μM, compared with micromolar values for the concentration in the CSF)[14,16] is found in certain glutamatergic neurons. It is proposed that labile pools of Zn^{II} and Cu^{II} are responsible for triggering the Aβ aggregation process or for the formation of Aβ aggregates of higher toxicity than the metal-free Aβ. Among the various intermediates in the aggregation process, soluble oligomeric forms are now considered to be the most toxic because of various events[17] including disruption of the synaptic function, effects on the integrity of the membrane bilayer, and production of ROS (reviewed in ref 18).

dx.doi.org/10.1021/ic4003059 | Inorg. Chem. 2013, 52, 12193−12206

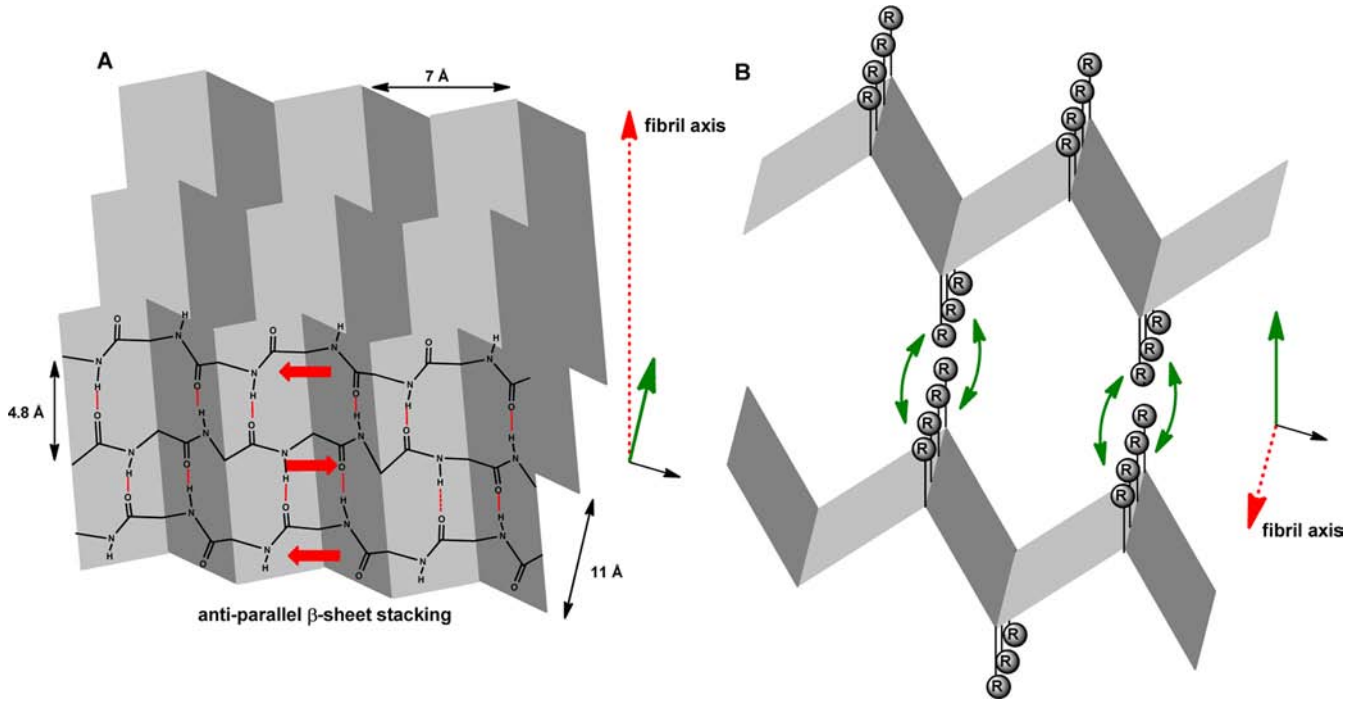

Figure 2. Scheme of the amyloid structure. (A) Hydrogen bonds between the backbone amide functions are shown by dotted red lines and are directed along the fibril axis. (B) Interactions between the side chains are shown by green arrows and are directed perpendicularly to the fibril axis.

2. STRUCTURES OF Aβ AND M^{N+}-Aβ

2.1. Aβ Structures without Metal Ions. *2.1.1. Monomer.* Monomeric Aβ is regarded as a disordered peptide, meaning that it is highly flexible and does not have a defined 3D structure.[19] Although soluble Aβ in aqueous buffer showed a circular dichroism (CD) spectrum typical for a predominantly random-coil conformation,[20,21] NMR analysis suggested that the peptide has a propensity to form a secondary structure, particularly at lower temperature.[22,23] A certain degree of structure has also been suggested from proteolysis-resistant segments (in particular Ala21−Ala31) in monomeric Aβ.[24] Thus, monomeric Aβ can be regarded as a disordered, highly flexible peptide, with a preference for some conformations. It is classed as an intrinsically disordered protein/peptide and considered to be a collapsed structure (which is distinct from denaturated and/or random coil).[25] In other environments, other conformations are possible. For instance, and perhaps most importantly, in a more hydrophobic environment (like an organic solvent or in the presence of detergent), the peptide adopts a structure with a high content of α-helicity.[26] This is of biological relevance because the peptide is likely to be in an α-helical structure when it is part of the APP and after cleavage of β- and γ-secretases.

2.1.2. Aβ Amyloids. Amyloids in general are aggregated proteins or peptides organized in β strands that are in the direction perpendicular to the fibril axis (cross-β-strands). They form β sheets, where the hydrogen bonds between the backbone *H*−N (of one strand) and *O*═C (of the neighboring strand) are in the direction parallel to the fibril axis. The strand can be a parallel or an antiparallel β sheet. The interactions (hydrophobic, salt bridges, etc.) between the side chains are in the direction perpendicular to the fibril axis (Figure 2).

Amyloids of Aβ are polymorphic. Several structural models, mainly based on solid-state NMR data, have been suggested. Two examples are shown in Figure 3. The C-terminal part of Aβ from amino acid residues around 10−13 up to 40/42 are in a β-sheet conformation with a turn in the middle. The N-terminal part is normally proposed to be flexible, although it might have some β-strand content.[27]

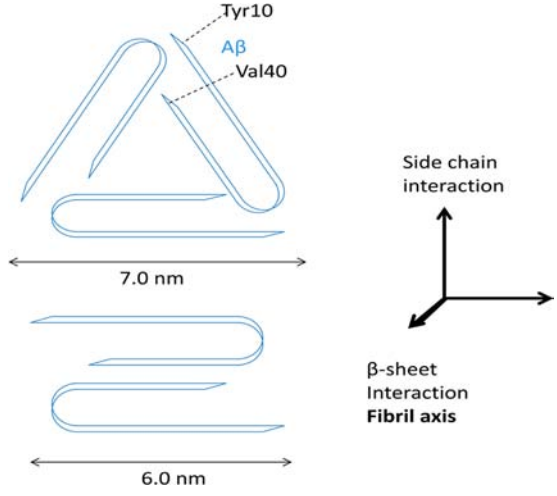

Figure 3. Two models of Aβ fibrils based on solid-state NMR constraints, exemplifying the polymorphism of Aβ fibrils. The scheme represents a cross section of the fibril, made of three (upper) or two (lower) Aβ. Aβ has two β strands with a turn. The fibril axis is perpendicular to the paper plane, and the peptides pile up by adding the same unit along the fibril axis via hydrogen bonds between the peptide backbone amides (adapted from ref 28).

2.1.3. Oligomers of Aβ. The term "oligomers" is often used for aggregation intermediates, meaning all intermediate species from the monomer to the mature amyloid fibril. However, often it is not clear if an intermediate is a "real" intermediate, i.e., on the way to the amyloid (on-pathway), or if it is an off-pathway structure that branches of the aggregation path from the monomer to the amyloid. Off-pathway intermediates,

dx.doi.org/10.1021/ic4003059 | Inorg. Chem. 2013, 52, 12193−12206

in contrast to on-pathway intermediates, will not aggregate further into fibrils.

Aggregation is a dynamic process, in which different aggregation states are in exchange. Thus, during aggregation, several states are simultaneously present. These intermediates are metastable. Hence, determination of a 3D structure is challenging because methods for structure determination require normally homogeneous and stable samples. Attempts to stabilize an intermediate for structural analysis might change the intermediate itself. Because the energy landscape is relatively flat, a small change can tip a conformer or an aggregation state over to another one.

Different oligomers have been described, starting from the dimer up to structures close to the mature amyloid.[29] So far, no structure with the atomic resolution of an Aβ oligomer has been reported. However, recently Stroud et al.[30] reported a model of a toxic oligomer (dubbed TABFO) based on several biophysical characterizations and their previous work on crystal structures of amyloidogenic peptides (but not crystals of amyloid fibrils; Figure 4).

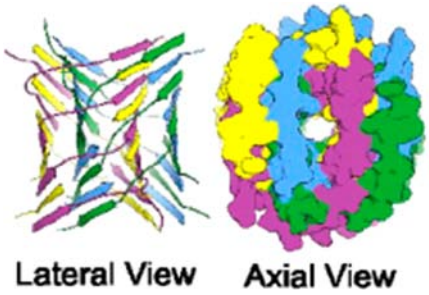

Figure 4. Model of the oligomer named TABFO (diameter ~8 nm) composed of 20 ordered Aβ42 peptides (taken from ref 30). In contrast to the fibrils, Aβ has no turn in the 23−28 region and strands form antiparallel sheets.

2.2. Aβ Structures with Metal Ions. *2.2.1. Monomeric Metal−Aβ Complexes.* Aβ is an disordered peptide that can adopt a multitude of different coordination sites with quite similar energies. The species are often in fast equilibria (milliseconds or faster) by ligand-exchange reactions. That means that subtle changes in the peptide sequence or other parameters (like pH) can have a dramatic impact on the population of the different species and the major species can change.[31] Similarly, the disordered peptide can adapt its structure to the structural and electronic requirements of the metal ion (in contrast to a well-structured metalloprotein, which can impose its binding site to the metal). As a consequence, the ligands and, hence, the peptide structure can substantially differ between two divalent metal ions. Thus, the understanding of how Cu^{II} and Zn^{II} affect the structure and dynamics of Aβ is just at the beginning and will be paramount to understanding how they modulate aggregation. This is not an easy task, considering the high flexibility of Aβ and the dynamics of its binding to Cu^{II} and Zn^{II}.

In the past decade, a huge number of studies have been reported regarding the coordination of metal ions of interest to the Aβ peptide, which have been recently reviewed in refs 32−35. The most accepted coordination models are reproduced in Figure 5. Briefly, for Cu^{II}, two components, usually noted I and II, coexist at pH 7.4. In I, the Cu^{II} site is preferentially made up of the $-NH_2$ terminal amine, the adjacent CO function from the Asp1−Ala2 peptide bond, the imidazole ring of His6, and the imidazole ring of His13 or His14, with the two latter His residues being in equilibrium for one equatorial binding position.[36] In the apical position, the involvement of a carboxylate has been proposed via direct interaction[37] or via a hydrogen-bonding network with a water molecule.[38] In II, the difference with I is due to deprotonation of the Asp1−Ala2 amide bond, leading to a Cu^{II} equatorially bound to the $-NH_2$ terminal amine, the adjacent deprotonated amide function from the Asp1−Ala2 peptide bond, the adjacent CO function from the Ala2−Glu3 peptide bond, and one imidazole ring of either His6, His13, or His14.[36] For Cu^{I}, the structure has been proposed to be a His−Cu^{I}−His motif, where two imidazole rings of His are linearly bound to the metal center.[32,36] It has also been suggested that His13−Cu^{I}−His14 is preferentially involved over His6−Cu^{I}−His13 and His6−Cu^{I}−His14.[39] For Zn^{II} and Fe^{II}, the situation is less clear, with several differing results on Zn^{II} and only one report for Fe^{II}. In a plausible model,[33,34] Zn^{II} is bound by the two or three imidazole rings of His residues, the carboxylate group from Glu11, and Asp1 either

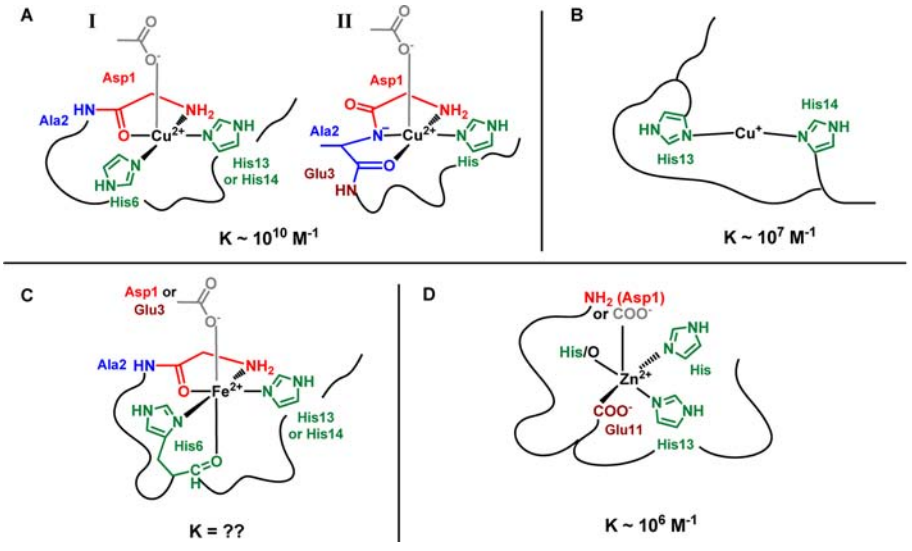

Figure 5. Proposed coordination sites of Cu^{II} (A), Cu^{I} (B), Fe^{II} (C), and Zn^{II} (D) ions to the soluble forms of Aβ peptide. *K* represents the apparent association constant of the metal ion and monomeric Aβ at pH 7.4 with 0.1 M salt but in the absence of a competing buffer.

dx.doi.org/10.1021/ic4003059 | *Inorg. Chem.* 2013, 52, 12193−12206

via the $-NH_2$ terminal amine or the carboxylate group.[40,41] For Fe^{II}, the only available model reports a coordination close to the one observed for component I of Cu^{II}, i.e., with the imidazole rings of His6 and of His13 or His14, the $-NH_2$ terminal amine, and the adjacent CO group, with the fifth and sixth positions being occupied by the CO group of His6 and a carboxylate group, preferentially that of Asp1 or Glu3.[42] In addition to the structural description of metal−Aβ complexes, another important parameter is the affinity of each ion for the Aβ peptide. Metal-ion affinity follows the order Cu^{II} (10^{10} M^{-1})[43] ≫ Cu^{I} (10^{7} M^{-1})[44] ≥ Zn^{II} (10^{6} M^{-1}),[35] with the affinity of Fe^{II} having not been evaluated. The values given represent the apparent association constant of the metal ion and monomeric Aβ at pH 7.4 with 0.1 M salt in the absence of a competing buffer.

Hence, binding sites are specific of metal ions in line with the electronic properties. However, coordination of those ions to the Aβ peptide shares a common feature, which is the dynamic binding of metal to the peptide and the associated equilibria between equivalent ligands for a binding position.[32,45]

2.2.2. Amyloids of Metal−Aβ. Cu^{II} coordination is generally the same as that in the monomeric structure, as proposed by advanced electron paramagnetic resonance (EPR) techniques.[46−48] A solid-state NMR study confirmed the implication of His13 and His14 (His6 was not site-specifically-labeled with ^{13}C and thus is not directly addressed) but also proposed carboxylates (C-terminal, Glu3,11, and/or Glu22 might be involved). Other residues are also possible because not all residues have been labeled and examined. Moreover, analysis suggested that Cu^{II} binding induced no major structural change in the β strands of hydrophobic core residues (18−25 and 30−36).[49]

A similar conclusion was made for Zn^{II}-Aβ aggregates, where Zn^{II} binding affected mainly the N-terminal part and the loop region but did not disturb the β strands. In this case, evidence for breaking of the salt bridge between Asp23 and Lys28 was obtained.[50] No details about the Zn^{II} ligands were obtained, apart from the involvement of His13 (the other potential ligands were not isotope-specifically-labeled and, hence, could not be observed). Thus, the Zn^{II} coordination sphere is ill defined, and only low-resolution or theoretical studies are available.[51,52]

The question of whether Aβ amyloids have a higher affinity for Zn^{II} and Cu^{II} than Aβ monomers has been addressed. This is of importance because it could explain why metal ions accumulate in amyloid plaques. For Zn^{II}, a 3−5-fold increase in the affinity has been reported for aggregates formed in the presence of Zn^{II}, but no increase was found for Zn^{II} binding to preformed amyloids.[53]

Cu^{II} affinity was considered to be independent of the aggregations state,[9,48] but a recent publication suggested a more than 10-fold increase in Cu^{II} and showed that aggregated Aβ is able to compete with human serum albumin (a native Cu^{II} binding protein occurring at high concentration in the brain) for Cu^{II} binding.[54]

2.2.3. Oligomers of Metal−Aβ. Very little is known about the coordination chemistry and peptide structure of metal−Aβ aggregation intermediates. EPR did not detect differences in Cu^{II} coordination during aggregation, suggesting that the Cu^{II}-binding mode is not altered.[48] Structural information on the intermediates relies mostly on microscopic studies [atomic force microscopy (AFM) and transmission electron microscopy (TEM)] and reports generally that Zn^{II} and Cu^{II} alter the amount and/or structure of the oligomeric species (Table 2, e.g., entries 1−5).

Regarding Cu^{I} bound to oligomers, a pioneering study by X-ray absorption spectroscopy (XAS) was recently reported.[55] In contrast to Cu^{I} coordination in the monomeric form (see section 2.2.1), in the oligomeric soluble forms, a tetrahedrally bound Cu^{I} was proposed, a geometry that is anticipated to trigger Cu^{I} reactivity toward dioxygen. However, the conclusions drawn from the XAS-only study should be confirmed by independent techniques.

3. AGGREGATION MECHANISMS

3.1. Aβ Aggregation without Metals. *3.1.1. Aggregation of the Aβ Peptide.* Monomeric Aβ peptides are the basic constitutive elements of amyloid fibrils: their self-assembly initiates fibril formation. However, this type of peptide has a strong tendency to randomly conglomerate into so-called amorphous aggregates.[56] In contrast to the well-ordered amyloid fibrils (see above), amorphous aggregates are unordered precipitates (Figure 6). We use here aggregation as an umbrella term for more ordered amyloid formation (fibrillation or fibrillization) or unordered precipitation in amorphous aggregates. The occurrence of amyloid fibrillation or amorphous aggregation is determined by the thermodynamic solubility of the peptide in water. Indeed, it was shown that amyloidogenicity depends on the peptide critical concentration (C_c), i.e., the peptide concentration relative to its solubility.[57−59] C_c of Aβ40 at 37 °C in phosphate-buffered saline (PBS) is in the range of 0.7−1 μM.[60] Note that this solubility refers to the thermodynamic minimum; the initial solubility of the Aβ powder in a buffer is higher but will lead to aggregation.

Thus, below the solubility limit, amyloidogenic peptides will, nevertheless, remain dissolved, while above the solubility limit, peptides will form amyloid fibrils or amorphous aggregates depending on the stability of the aggregated forms and/or the kinetics of their formation. Environmental factors such as the pH and temperature also have an impact on the peptide fibrillation or precipitation.

Metal ions could have an impact on amyloid formation by either promoting another pathway (off-pathway, like amorphous aggregate formation) or modulating the on-pathway, thermodynamically or kinetically. They could thermodynamically favor amyloid fibrils by either destabilizing the monomers (increase of their energy) or stabilizing the amyloids (decrease of their energy). Metal ions could accelerate the kinetics by either stabilizing the nucleus (transition state) or destabilizing the monomer.

3.1.2. Amyloid Fibril Formation of Aβ. The assembly of Aβ monomers into highly ordered fibrils is a complex and dynamic process that involves multiple self-assembly steps. In particular, Aβ peptides undergo complex conformational changes, aggregation, and reorganization to form characteristic cross-β-sheet fibrils.[62] As described for classical protein aggregation, it was shown that amyloid formation proceeds efficiently only under conditions where the native state is destabilized.[63] Such a destabilization is not necessary for Aβ because it is a disordered peptide. Both thermodynamic and kinetic factors are involved in amyloid aggregation, and distinct intermediate forms can coexist at each stage of the process (Figure 7).[64] Different paths involving these transient intermediates (both ordered and disordered) have been described or hypothesized in the literature. A general agreement has been reached regarding a basic underlying aggregation mechanism: formation and polymerization of amyloid fibrils rely on successive nucleation and elongation steps. The reaction kinetics is controlled by two key parameters, nucleation (k_n) and elongation (k_e) rate

dx.doi.org/10.1021/ic4003059 | Inorg. Chem. 2013, 52, 12193−12206

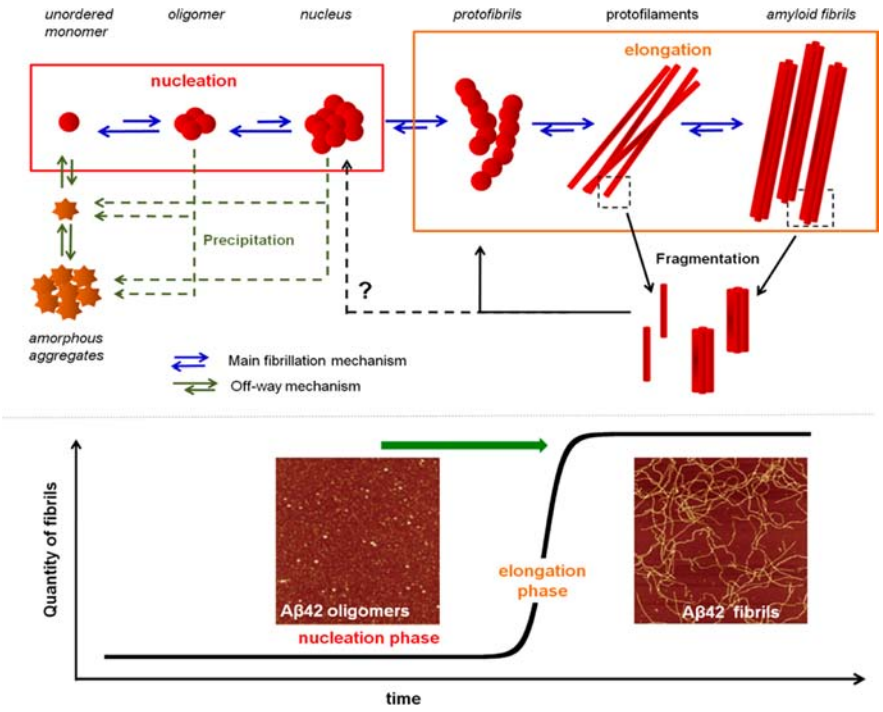

Figure 6. Schematic representation of amyloid aggregation paths (top section) and AFM images (2 × 2 μm from ref 61) of the Aβ peptide at the oligomeric and fibrillar stages superimposed with the typical sigmoid curve of fibril formation often revealed by ThT fluorescence (bottom section).

constants. However, more complicated scenarios and different kinetic models have been proposed (for review, see ref 70).

Nucleation. According to the generally accepted model, unstructured monomers in solution cluster and form nuclei ("nucleation phase" or "lag phase"). Formation of these transient nuclei requires a series of association steps that are thermodynamically unfavorable because the resultant intermolecular interactions do not surpass the entropic cost of association.[65] Consequently, nuclei generation represents the limiting step of fibril production, and a lag time is observed before aggregation can proceed further to the elongation phase. Newly formed nuclei will then either decay back to the ground state and serve in the formation of new fibrils or join ever-lengthening fibrils.[64,66] Several types of nucleation mechanisms have been suggested. They differ, for instance, in the oligomeric state of Aβ that associate (monomer, dimer, trimer, etc., addition) or at which oligomeric state conformational changes occur (Figure 8).

Elongation. Once nuclei have been generated, they serve as a template for binding and conformational transitions of monomeric or oligomeric proteins. Fibrillar assemblies start to form, which gives rise to the abruptly accelerated elongation phase (Figure 6 gives a general schematic representation).[67]

This elongation phase represents the major step during which intermediate states acquire β-sheet structures, leading to mature amyloid fibrils (Figure 8). This enrichment in β-sheet secondary structures, and thus the actual fibrillation process, can be routinely probed by fluorescent dye-binding assays and, in particular, the ThT binding assay (Table 1 and Figure 6).[68] Indeed, upon binding to the peptide assemblies, this dye displays distinct spectral properties compared to its native, unbound state. The slow nucleation phase, during which low β-sheet content is present in Aβ monomers, only causes small interactions between ThT and the peptide, while the fast-occurring elongation phase (involving fast-increasing β-sheet amounts) clearly causes a steep increase in dye–peptide binding before reaching a plateau (Figure 6).

Fragmentation. Computational analysis of data obtained from several amyloidogenic systems argues that the sole nucleation–polymerization mechanism is not sufficient to justify the kinetic data obtained for these systems.[69] Including fragmentation improved the fit. Fragmentation of fibrils leads to an increase of the number of fibrils (or nuclei) and hence accelerates overall elongation (Figure 6).

3.2). Aβ Aggregation with Metal Ions. Here we discuss mainly Zn^{II} and Cu^{II}, which are the most studied metals. Cu^{I} and Fe^{II} are difficult because they have to be studied in anaerobic conditions to avoid oxidation. Fe^{III} is not soluble (and precipitates as hydroxides), even when bound to Aβ, thus making analysis difficult.[41]

Metal ions can impact aggregation in two ways, either by binding and subsequent structural changes, without covalent modification (only coordination bonds) or by peptide modification. Redox-active $Cu^{I/II}$ and $Fe^{II/III}$ can indeed lead to constitutional changes, via the catalysis of ROS production that attack the peptide (for a recent review, see ref 13). For instance, stable dimers seem to be physiologically relevant, in particular via the covalent formation of dityrosine,[71] but we focus here on the first type of metal-ion impact.

The impact of metal ions can be considered on different levels:[9,72] (i) metal specificity; (ii) comparison of amyloid versus amorphous aggregates; (iii) comparison of kinetics versus thermodynamics; (iv) impact of metal binding on nucleation and/or elongation; (v) whether metal binding can change the aggregation pathway or not.

3.2.1. Metal-Ion Specific Effect on Aβ Aggregation. Metal ions vary in their coordination chemistry. The most commonly studied ions to date, Cu^{II} and Zn^{II}, bind to Aβ differently (see section 2.2.1), generating diverse peptide structures, which thus has an impact on amyloid formation. Indeed, most of the

dx.doi.org/10.1021/ic4003059 | Inorg. Chem. 2013, 52, 12193–12206

Table 2. Overview of the Literature Concerning the Impact of Metal Ions (Mainly Cu^{II} and Zn^{II}) on the Aggregation of Aβ[a]

metal ion	peptide	ratio of M^{n+}:Aβ	measure of aggregation	conditions	observations and/or conclusions	entry	ref
Zn^{2+}	Aβ40	2:1	TEM, CD, ThT, cell toxicity	10 μM Aβ	Zn stabilized a toxic oligomer (after 2 h) estimated as 20 Aβ (diameter ~11 nm), β sheet, less ThT fluorescence (oligomer different from apo-Aβ)	1	92
Zn^{2+}	Aβ40	various	centrifugation and filtration followed by radiolabeled Aβ, amino acid analysis, and immunoassay	different (salt, proteins, etc.)	≥100 μM needed for aggregation	2	101
Zn^{2+}	endogenous Aβ	various	quantitative western blot and ELISA	CSF	EC50 ~0.13 mM Zn^{II} for aggregation	3	102
Zn^{2+}	Aβ40	various	determination of critical Aβ concentration (C_c) by sedimentation	4 μM Zn^{II} in PBS	with 4 μM Zn^{II} in PBS; soluble Aβ was diminished by 11% (from 15 μM)	4	74
Zn^{2+}	Aβ40	1:1	TEM, FTIR, ThT, N−H exchange, critical concentration, etc.	250 μM Aβ PBS	(i) lower ThT binding (intensity); (ii) higher H−D exchange; (iii) slightly higher C_c; (iv) TEM, less mature fibrils; (v) with Zn^{II} similar overall structure (β sheets) but more loosely	5	75
Zn^{2+}	Aβ40	1:2, 1:1, 2:1	time-resolved Tyr fluorescence; light scattering, XAS, TEM, etc.	50 μM Aβ	Zn^{II} induced rapidly ($t1/2$ of 0.02−1 s); with Zn^{II}, no mature fibrils, stabilized oligomers; XAS suggests that Zn^{II} coordination changes between 2 and 500 ms	6	107
Zn^{2+}	Aβ42	1:1	solid-state NMR and TEM	400 μM Aβ42 and Zn^{II}	(i) TEM shows less fibrillar structure with Zn^{II}; (ii) Zn^{II} binding affects mostly the N-terminal part(1−16) and loop region (23−28) but not the cross-β-structure of the two β strands; (iii) Zn^{II} breaks the salt bridge between Asp23 and Lys28; (iv) Zn^{II} interacts with His13 (other His not ^{15}N labeled)	7	50
Cu^{2+}	Aβ42	1:10, 1:1, 10:1	SDS and native PAGE, ThT, TEM, SEC, light-scatter cell toxicity	10 μM Aβ Cu^{II} in form of Cu^{II}-Gly	substoichiometric Cu^{II}: amyloid aggregates supra: small spherical oligomers (high light scattering, more di-Tyr)	8	93
Cu^{2+}	Aβ40 (and 16, 28, and 42)	0−5 Mainly 0.25; 1 and 5	ThT, MS, AFM, SEM, capillary electrophoreses	40 μM Aβ	distinct pathways depending on the Cu^{II}:Aβ ratio: (i) shift from fibrillate to nonfibrillar with increasing Cu^{II}:Aβ ratio; (ii) spherical aggregates (AFM, diameter 10−100 nm) as the end point for all Cu^{II}:Aβ ratios, also partly observed for apo-Aβ	9	78
Cu^{2+}	Aβ42	20:1	ThT, congo red, TEM	8 μM Aβ	Cu^{II} reduced ThT and CR; TEM showed spherulites (no fibrils)	10	105
Cu^{2+}	Aβ42	1:1	ThT intensity, AFM	from pH 5 to 9	Cu^{II} inhibits fibrils (spheres formed)	11	108
Cu^{2+}	Aβ40, Aβ16	0−1	NMR relaxation, time resolved Tyr fluorescence, and light scattering	300 μM Aβ, 40 μM Aβ	formation of a transient dimer Aβ-Cu^{II}-Aβ, which is off-pathway from amyloid formation	12	82
Zn^{2+}, Cu^{2+}	Aβ40	various	fluorescence correlation spectroscopy	60 μM Aβ (spiked with 0.1 μM rhodamine labeled)	1 μM Cu^{II} and 4 μM Zn selectively removed oligomers (20−130 nm); 30 μM Cu^{II} and 600 μM Zn^{II} lead to precipitation	13	94
Cu^{2+}, Zn^{2+} (Fe^{3+}, Al^{3+})	Aβ40	from 0.2 to 25	CD, ThT, TEM, dot blot, PICUP, etc.	25 μM Aβ	(i) Zn^{II} and Cu^{II} increased oligomers (2−6mers; PICUP); (ii) Cu^{II} inhibited amyloids (ThT in intensity and time); (iii) 0.2−8 equiv of Zn^{II} largely reduced the ThT intensity but had a small fast increase; 1 equiv of Zn^{II} increased the oligomers (A11 antibody) in the first hours (but not 0.2 equiv)	14	95
Cu^{2+}, Zn^{2+}	Aβ42	1:100−1000	AFM	100 μM Aβ	(i) largely substoichiometric of Zn^{II} and Cu^{II} addition inhibited fibril formation; (ii) with Zn^{II}, small globular aggregates were formed; (iii) with Cu^{II}, ill-structured microaggregates were formed	15	96
Zn^{2+}, Cu^{2+}	Aβ42	0.3−3	AFM, FTIR, ThT	Aβ immobilized on solid surfaces	Zn^{II}: mostly amorphous aggregation Cu: at 3:1, stoichiometry amorphous at ≤1:1, mostly fibrils	16	97

dx.doi.org/10.1021/ic4003059 | Inorg. Chem. 2013, 52, 12193−12206

Table 2. continued

metal ion	peptide	ratio of M^{n+}:Aβ	measure of aggregation	conditions	observations and/or conclusions	entry	ref
Cu^{2+}, Zn^{2+}	Aβ40	various	ThT intensity and $t_{1/2}$, TEM, cell toxicity	5 μM Aβ and 160 mM NaCl for aggregation	0.2−1 equiv of Cu^{II} accelerated amyloid formation (ThT); Max ∼0.4	17	98
				2.75 or 10 μM Aβ for cell toxicity	substoichiometric Cu^{II}-Aβ was most toxic to cells (more than ≥1:1 and apo)		
					3 μM Zn^{II}: inhibited amyloid formation (ThT)		
Zn^{2+}, Fe^{3+}, Al^{3+}	Aβ40	1−1000 (0.1 −1000 μM)	sedimentation	100 pM ^{125}I-labeled Abeta 40 0.1% BSA added or CSF	sedimentation at ≥100 μM metal (with BSA) and at 1 mM in CSF	18	99
Zn^{2+}, Cu^{2+}, Fe^{2+}	Aβ40	100:1	native and SDS gel; AFM; congo red	10 μM Aβ, PBS; pH 5; pH 7.4	two different aggregation paths: (i) apo-Aβ at pH 7.4, nonfibrillar; (ii) apo-Aβ at pH 5 and Cu^{II}/Zn^{II} Aβ at pH 7.4, fibrillar	19	100
Zn^{2+} (Cu^{2+})	Aβ40	20:1	sedimentation and peptide in supernatant dosed by coomassie blue	2.5 μM Aβ	(i) Zn^{II}-induced aggregation of Aβ; (ii) Cu^{II} reduced this Zn^{II}-induced aggregation	20	103
Zn^{2+}, Cu^{2+}	Aβ40	excess metal	filtration 0.2 μm	^{125}I-labeled Aβ40 1.6 μM	Zn^{II} above 0.3 μM induced aggregation; 3 μM Cu^{II} induced some aggregation	21	104
Zn^{2+}, Cu^{2+}	Aβ42	0−5	ThT kinetics; separation by centrifugation at 10000g; TEM; cell viability	5 μM Aβ; 3.3 or 15 μM ThT	(i) Zn^{II} and Cu^{II} inhibited aggregation (ThT), increased the nucleation phase, and decreased the ThT intensity (plateau); (ii) slight decrease in the elongation rate; (iii) Zn^{II} and Cu^{II} induced precipitation	22	77
Cu^{2+}, Zn^{2+}	Aβ40/42	2:1 (mostly)	ThT kinetics and intensity; light and electron microscopy, CD, cytotoxicity, etc.	1−50 μM	Zn^{II} and Cu^{II} induced aggregation but not into amyloid fibrils; these nonamyloid aggregates were less cytotoxic	23	106
Zn^{2+}, Cu^{2+}	Aβ40	Zn^{2+} 0.3:1	mainly NMR	130 μM Aβ at 3 °C	(i) Zn^{II} binding induced aggregation (oligomers); (ii) apart from the N-terminal 16 aa, where Zn^{II} binds, Zn^{II} binding induced changes around Phe20 in the monomeric complex (before aggregation); (iii) order of disappearance of signals: 10−21, then 32−40, then 22−30	24	86
		Cu^{2+} 1.4:1	mainly NMR	30 μM Aβ at 3 °C	order of disappearance of signals: 32−40, then 22−30 (10−21 not detected)		
Cu^{2+}, Zn^{2+} (Al^{3+}, Fe^{3+})	Aβ42	10:1	ThT intensity; TEM; monomer concentration by HPLC	1 μM Aβ	(i) Zn^{II} and Cu^{II} inhibited amyloid formation; (ii) metal contaminants (Fe and Al) increased amyloid formation	26	109
Cu^{2+}, Zn^{2+}, Fe^{3+}	Aβ42 (40)	0.5:1	turbidity; ThT and congo red; SDS-PAGE	2 μM Aβ42; metals in the form of Cu^{II}- Gly or Zn^{II}-His; Fe^{III}-citrate	chelator DTPA inhibited amyloid formation of Aβ42. and Aβ42 initiated Aβ40 aggregation: a trace amount of metal ions can trigger Aβ42 aggregation	27	110

[a]This is not an exhaustive table. We tried our best to select the studies that focused on the aggregation mechanism.

dx.doi.org/10.1021/ic4003059 | Inorg. Chem. 2013, 52, 12193−12206

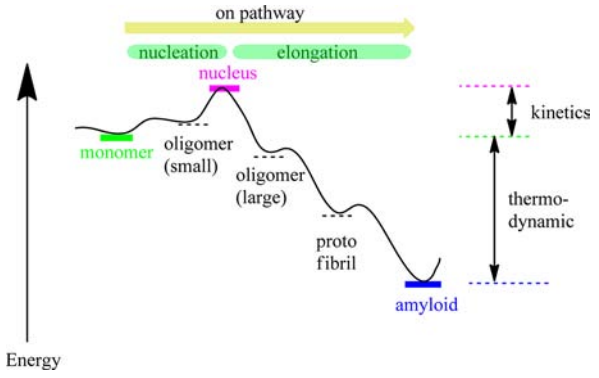

Figure 7. Schematic reaction coordinate for the formation of amyloids (blue) from monomers (green). The nucleus (purple) is considered the high-energy state, from which onward the reaction is downhill. The nucleus is the least populated state. A metastable intermediate can occur before or after the nucleus. They would be transiently populated. Here only species on the on-pathway are shown (faint brown arrow). Other oligomers or amorphous aggregates, could occur via an off-pathway.

studies report a difference in the structure, kinetics, and intermediates between Zn^{II}- and Cu^{II}-Aβ aggregation (Table 2, entries 14−17, 20, 21, and 23).

3.2.2. Amorphous (Precipitation) versus Amyloid. The distinction between the formation of amyloid-type aggregates and amorphous aggregates (precipitation) becomes important in the presence of metal ions because the addition of polyvalent metal ions is a classical method to precipitate proteins and other biomolecules.[73]

Indeed, a survey of the literature (Table 2, entries 8, 13, and 16−18) mostly agrees (but see entry 19) that high (classical 0.1 mM and more) or superstoichiometric Cu^{II} and Zn^{II} inhibit amyloid formation but promote precipitation of Aβ. However, this does not mean that no oligomeric structures or other forms can be observed during the aggregation process (Table 2, entry 8). Moreover, several studies reporting metal-induced aggregation used sedimentation or filtration methods not allowing the distinction between amorphous and amyloid aggregates (Table 2, entries 2, 3, 20, and 21).

3.2.3. Impact of Metal-Ion Binding on the Thermodynamics of Aβ Aggregation. The first consideration is to determine whether metal ions have an impact on the kinetics and/or thermodynamics. Thermodynamically, the metal-ion binding could stabilize or destabilize the monomeric species and/or amyloid fibrils (Figure 7).

This has often been determined by measuring the amount of amyloid fibrils in the presence and absence of the metal ion. However, one has to be sure that the aggregates are amyloid fibrils and that the aggregation is finished (thermodynamic equilibrium). A better way to address the thermodynamic stability compared to the crude sedimentation/filtration is determination of the critical concentration C_c, i.e., minimal concentration that leads to amyloids, which is equal to the concentration of monomeric Aβ in the presence of amyloid at equilibrium.

$$n(\text{monomeric A}\beta) \underset{k_{off}}{\overset{k_{on}}{\rightleftarrows}} \text{amyloid } (\text{A}\beta)_n$$

C_c can also be expressed as equal to k_{off}/k_{on}

This was developed by Wetzel and colleagues for apo-Aβ, in which they ascertained that they reached equilibrium by obtaining the same C_c when starting from a pure monomeric sample and from a pure amyloid sample.[64] As mentioned, this method relies on a relatively simple fast equilibrium between only two forms, monomeric Aβ and amyloid Aβ. Depending on the proposed aggregation mechanism, this might not be the case.[25]

Not much data in this respect have been reported. Sengupta et al.[74] (Table 2, entry 4) measured the critical Aβ concentration in the presence of Zn^{II} and found that, in substoichiometric Zn^{II} concentration (more could not be added

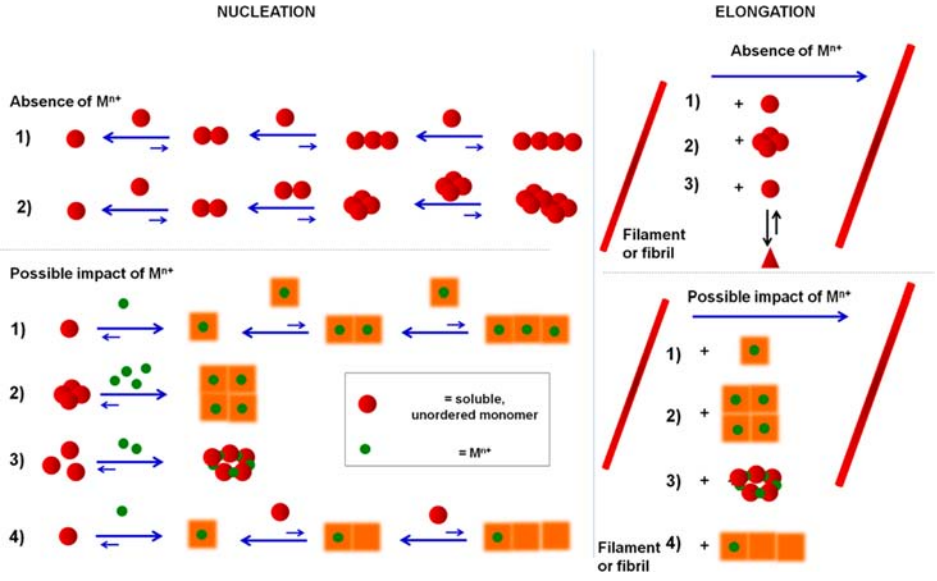

Figure 8. Left: nucleation step. Top: Soluble monomers could aggregate via different additions either by subsequent monomer addition (1) or by the addition of oligomeric species (2). Bottom: Metal ions could have an impact by forming a complex and changing the structure of the monomer (1) or an oligomer (2) or by bridging the monomers (3). Another important factor is the lability of metal-ion binding, which could allow catalytic action in the nucleation (4). Right: Elongation step. Top: Growth of filaments or fibrils can occur via the addition of monomer (1), oligomer (2), or a low populated state (3) in equilibrium with the monomer. Bottom: Impact of metal interactions via binding and changes of the structure for monomer (1) or oligomer (2), clustering of the monomer by bridging metals, or catalytic action.

dx.doi.org/10.1021/ic4003059 | *Inorg. Chem.* 2013, 52, 12193−12206

because they used PBS, and Zn^{II} would have precipitated as $Zn^{II}PO_4$), the critical concentration is almost the same. In another work, a slight but not significant change in C_c in the presence compared to the absence of Zn^{II} was found [C_c = 1.06 ± 0.18 (no Zn^{II}) and 1.36 ± 0.15 μM (with Zn^{II}); Table 2, entry 5].[75]

In principle, the amount of amyloid formation could be deduced from the ThT intensity at the end of the aggregation process (plateau) under the conditions that ThT is not limiting. However, this is critical for several reasons: (i) M^{n+} could quench the fluorescence (particularly paramagnetic Cu^{II}), although this does not occur in Aβ; (ii) M^{n+} could compete for the same binding site as ThT or M^{n+} could form different amyloid structures that differ in the number or type of ThT binding sites. Indeed, a more than 4-fold decrease of the ThT intensity with Zn^{II} was reported, although C_c and other parameters did not change much.[75]

It is astonishing that not more detailed work has been done to address this question. This might come from the idea/assumption that metal ions (Zn^{II} and $Cu^{I/II}$) have an impact mostly on the aggregation kinetics.

3.2.4. Impact of Metal-Ion Binding on the Aggregation Kinetics of Aβ. a. General Considerations and Problems. There are a multitude of studies reporting an effect of metal ions on the kinetics of Aβ aggregation (Table 2). The results seem very confusing, because for the most studied metal ions, Cu^{II} and Zn^{II}, promotion and inhibition of aggregation were documented. Often this fact is commented by "the effect of metal ions depends on the experimental conditions", and then the issue is considered closed. However, very little effort has been made to see whether reproducible results can be obtained under the same experimental conditions by different groups. Even when experiments were repeated at the very same conditions, different results could be obtained. In that case, the batch of peptides can be blamed ("batch dependent"). Of course, these are far from ideal conditions to make progress in the field. It seems that it is really a difficult question, but there are several points that can be taken into account to improve the situation: (i) distinction between the types of aggregates (amyloid of amorphous); (ii) metal to Aβ ratio; (iii) concentrations; (iv) pH; (v) buffer, salt, temperature, stirring, etc.; (vi) starting material and treatment of the peptide before aggregation experiment.

Whereas the first five points are straightforward to address,[76] the last one is difficult because batches are indeed different and the preparation can result in different starting materials. The problem seems to be the presence of different amounts and/or types of preaggregated peptides, which can nucleate the aggregation. The only way around that is to use pure monomeric peptide as the starting material. An obvious way to do that is to pass Aβ over a size-exclusion chromatograph and collect the monomeric fraction.

Another point is that often aggregation is monitored by only one method. It is very important that, whenever possible, several methods in parallel are used because each method has its advantages and its limitation (Table 1).

To gain mechanistic insight into the effect of metal ions on Aβ aggregation, defined stoichiometries seem more appropriate. The estimation of the metal content in amyloid plaques suggests that the metal content is substoichiometric, and hence focus should be on a M^{n+}-to-Aβ stoichiometry of ≤1. A justification might be when it is intended to simulate native concentrations (like for the CSF) where very low Aβ concentrations are present (nanomolar), but then one has to consider the presence of several potential metal ligands in biological media, and hence a lower availability of "free" or "loosely bound" metals.

Here, we mainly consider a metal-to-Aβ ratio of ≤1 because the focus is on the mechanisms of aggregation.

b. Impact of Metal-Ion Binding on the Nucleation–Elongation Framework. Metal binding could have an impact on the nucleation, elongation, and/or fragmentation phases (Figure 8). To the best of our knowledge, there is no report on the impact of metal ions on fragmentation. For the elongation process, a reduction was reported for Cu^{II} and Zn^{II} on Aβ42[77] (Table 2, entry 22). A factor of 2 was observed for the addition of ∼0.5 Zn^{II} per Aβ42. The main impact of Zn^{II} and Cu^{II} was mostly reported on the nucleation phase in this study,[77] in line with most of the other reports (Table 2, entries 6, 12, and 14). The same study reports also the inhibition of ThT fluorescence and hence inhibition of amyloid fibril formation; Cu^{II} and Zn^{II} thus induced fast assembly into amorphous aggregates. An important finding was that these rapidly obtained amorphous aggregates (induced by Zn^{II} or Cu^{II}) can convert slowly to amyloid fibrils (as assessed by TEM), indicating that amyloid fibrils are thermodynamically more stable than the amorphous aggregates. Moreover, this might also explain the discrepancy of different studies reporting inhibition or promotion of amyloid fibrils in the presence of Zn^{II} and Cu^{II}, as well as differences in cell toxicity.[77] However, another study[78] suggested that amyloid fibrils of apo-Aβ40 can partially progress into spherical structures (diameter 10−100 nm). Similar spherical structures were observed as the end point for different Cu^{II}-to-Aβ40 ratios.

The exact route of how metal ions affect the nucleation and elongation processes is not known: Nucleation could be affected by changing the energy of the nuclei (highest energy transition state; Figure 7), but also monomer stability can impact the kinetics. This could occur by a metal-induced conformational change or population shift or by binding between two Aβ molecules (bridging metal ion), which can bring Aβ closer and therefore promote aggregation (Figure 8). Elongation could be affected by (de)stabilizing conformers that fit better or worse with docking on the fibril end. A catalytic way is also imaginable, where metal binding helps just to add the monomer, but once it is added to the fibrils, it leaves again. In the first case, elongation would need stoichiometric amounts of metal per Aβ (or 0.5 equiv if M^{n+}-Aβ_2 is added). In contrast in the latter case, substoichiometric amounts of metal ions would be enough (Figure 8).

In conclusion, there is no clear or drastic difference in the underlying nucleation/elongation mechanism for forming Aβ fibrils between apo-Aβ and Cu^{II}/Zn^{II}-Aβ. The difference seems to be in the kinetics and intermediates (structure and stability) because the final mature fibrils are rather similar (also an extension of the nucleation/elongation, e.g., by including a conformation change of an aggregated state).

3.2.5. Impact of Metal-Ion Binding to Aβ on the Overall Charge. The overall charge is an important parameter for aggregation because generally aggregation is faster when the overall charge approaches 0, and hence the highest aggregation rate for Aβ is observed around the isoelectric point of ∼5.5.[79] Metal-ion binding can induce changes in the overall charge. By studying an amyloidogenic model peptide under relatively fast aggregating conditions (start after several minutes), we found a tendency to promote precipitation when the net charge equals

0, whereas amyloid formation was promoted when the net charge was more positive (~2+).[80] However, this might change for other peptides like Aβ or under less aggregating conditions (see the Conclusions and Perspectives section).

Cu^{II} and Zn^{II} are both charged 2+, whereas Aβ is at pH 7.4 and charged about 3−. Thus, complexes of Cu^{II}- and Zn^{II}-Aβ would have a net charge of 1− and would hence be more prone to aggregation. However, to obtain the overall net charge, one has also to consider the protons that are displaced by the metal ion. Cu^{II} is a better Lewis acid than Zn^{II} and can better replace protons. In contrast to Zn^{II}, Cu^{II} is able to deprotonate amides in Aβ (see Cu^{II} coordination, component II, above). This might suggest that Zn^{II} could be more efficient in inducing aggregates of Aβ because Zn^{II} binding yields a complex closer to the net charge 0 than Cu^{II} binding. However, this might only be true for higher Aβ concentrations because the binding affinity also comes into the play. The apparent dissociation constant for Zn^{II} is in the micromolar range. That means, at low micromolar Aβ and metal concentrations, Zn^{II} will only bind partially to Aβ, whereas Cu^{II} will bind almost completely. However, as mentioned above, the fact that these metal ions are labile enables them to interact with the entire pool of Aβ.

3.2.6. Cu^{II}- and Zn^{II}-Bridged Dimers. An attractive possibility to promote aggregation by metal ions is the formation of metal-bridged dimers because a dimer is the first step toward aggregation. It is clear that the main complex before aggregation is a 1:1 complex for Cu^{II}- and Zn^{II}-Aβ (see section 2.2.1) and (at least for Cu^{II}) that such dimers exist transiently.[81] However, Pedersen et al. suggested that they are not precursors of aggregation.[82] Whether Aβ is bridged by Cu^{II} and Zn^{II} during aggregation is not clear. Considering the dynamics of metal binding (even in the aggregated state)[53,83] and that the N-terminal part is quite flexible, transient metal bridging seems likely. However, whether in an aggregated state bridged metals are the major state is unclear. EPR did not detect differences in Cu^{II} binding between the monomeric and aggregated states.[46,48,84] However, an increase in the binding constant was recently reported.[54] In the case of Zn^{II}, the main arguments come from calculations and XAS.[51,52] It seems that Zn^{II} has a higher tendency to form bridges because of the more flexible coordination geometry.

3.2.7. Summary in the Form of a Possible Scenario of How Zn^{II} and Cu^{II} Could Modulate Aβ Aggregation. It is relatively clear from the literature that Zn^{II} and Cu^{II} bind rapidly to monomeric Aβ and form first a monomeric M^{II}-Aβ complex.[82,85,86] This is the major complex, but transiently metal-bridged dimers (Aβ-M^{II}-Aβ) are formed via the fast exchange of M^{II} between peptides (milliseconds or faster), but for Cu^{II}, those dimers likely are not precursors of the aggregates (off-pathway).[82] NMR suggests also a fast exchange for Zn^{II},[87] probably via metal-bridged dimers. Whether they are also off-pathway is not clear.

Zn^{II} and Cu^{II} binding to the N-terminal 1−16 stretch induces also changes in the rest of the peptide (17−40/42). NMR of Zn^{II} and Cu^{II} binding to Aβ40 showed changes in the dynamics around Phe19−Phe20, which are supposed to be the initiators of aggregation (first contact region between two Aβ).[86] Zn^{II} binding to Aβ40 induced a relatively rigid turnlike structure at residues Val24−Lys28, whereas the residues flanking this region become more mobile in the picosecond to nanosecondtime scale.[88] The turn structure has been recognized as an important feature in aggregation because it could serve as a nucleation site.[24] As mentioned above, changes in the overall charge upon binding of Zn^{II} and Cu^{II} might play a role. It is reasonable to assume that they do and they give a kind of underlying driving force, but it cannot explain the very specific effect of the different divalent metal ions (like Cu^{II} vs Zn^{II}).

After rapid Zn^{II} and Cu^{II} binding, their subsequent structural and dynamic changes lead to a more aggregation-prone structure. A possibility might be an interpeptidic contact in the central hydrophobic region (around Phe19/20)[86] or a turnlike structure at residues Val24−Lys28, bringing together the two hydrophobic parts around Phe19/20 and -32−40.[88] This might stabilize structures closer to a β sheet and hence promote aggregation. However, quite different scenarios are conceivable, and some support can be found in the literature. For instance, a partially α-helical structure has been observed in Aβ aggregation and proposed to be an intermediate.[89] An indication that this intermediate might also play a role in the aggregation of Zn^{II}- and Cu^{II}-Aβ has been reported.[90,91]

4. CONCLUSIONS AND PERSPECTIVES

The present review focused on the impact of metal ions on the aggregation of the peptide Aβ. Although the aggregation is not easy to control and reproducibility is a problem, even in the absence of metal ions, there seem to be some trends that are in agreement with most of the studies, at least for Cu^{II} (Table 2).

A too fast aggregation will lead to amorphous aggregates; for the formation of amyloids, more time is needed to acquire a more ordered structure. That means, at low concentration, a peptide with a lower propensity to aggregate and/or a low metal concentration favors amyloids, whereas at high concentration, peptides with a high propensity to aggregate and/or a high metal−peptide stoichiometry will favor precipitation. This might also be extended to the pH: the closer the pH is to the pI, the more precipitation occurs. Too far away from the pI will stop aggregation. Also the salt concentration is likely such a factor; very low or very high would promote precipitation.

In other words, distinction is made mainly by the speed of aggregation; a too fast aggregation favors precipitation (like high concentration, Aβ42 compared to Aβ40, high Cu^{II} or Zn^{II}, pH close to pI, etc.), whereas a too low concentration, pH too far away from pI, can stop aggregation altogether.

Although it is clear that the metal ions affect the aggregation in a metal-specific way and the highest impact is on the nucleation phase and the amount and/or structures of oligomers, there is a tremendous amount of work to do for determining the impact of metal ions on the aggregation mechanism on a molecular level. Nevertheless, the gained insight might help to design and test potential therapeutic molecules based on the interaction of Aβ with metal ions. Encouraging results were obtained by chelators with ionophoric activity during the past decade.[111,112] This triggered a multitude of developments and studies of Cu^{II} and Zn^{II} chelators.[113,114]

As shown above, the labilities of Cu^{II} and Zn^{II} ions are linked to their involvement in triggering Aβ aggregation. Hence, another possible therapeutic route relying on the preclusion of Aβ aggregation may rely on $Cu^{I/II}$ and Zn^{II} replacement by kinetically inert ions such as Ru^{II}, Pt^{II}, or Rh^{III}. At present, the first data obtained with such second- and third-row metal complexes are very promising.[18,115−120]

In conclusion, the interaction of metal ions with amyloidogenic peptides such as Aβ, prion, α-synuclein, IAPP/amylin,[9] etc., is an exciting field with a large scope for inorganic chemists, going from the design and synthesis of chelators up to analysis of the metal amyloidogenic peptides in a biological

environment. A molecular and quantitative approach of chemical sciences is needed to study rigorously the very tricky and dynamic aggregation of amyloidogenic peptides in the presence of metal ions.

AUTHOR INFORMATION

Corresponding Author

*E-mail: peter.faller@lcc-toulouse.fr.

Notes

The authors declare no competing financial interest.

ACKNOWLEDGMENTS

We thank all of the collaborators (in-house and externally) for their research and discussion, which is the basis of this article. Dr. B. Alies (LCC Toulouse) is acknowledged for helpful discussions. Research related to the review was supported by the "Region Midi-Pyrenees" (Research Grant APRTCN09004783). O.B. is supported by the French ANR "GRAL" (Agence Nationale de la Recherche Grant ANR-12-BS07-0017-01).

NOMENCLATURE

Definitions

aggregation = formation of aggregates, i.e., of polymers (starting from dimers) without a distinction of the type or structure (e.g., amorphous or fibrillar)

precipitation = formation of amorphous aggregates with no ordered structure

fibrillation = formation of amyloid aggregates showing a typical amyloid structure (ordered cross-β-strand structure)

mature amyloids = assumed end point of amyloid formation

oligomers = formed between a monomer and an amyloid; term often used for the small aggregates

protofibrils = aggregates assumed to be on the pathway to fibrils; shorter, rougher, "wormlike" structure

Abreviations

Aβn = amyloid-β peptide spanning to residues n

AFM = atomic force microscopy

AD = Alzheimer's disease

APP = amyloid precursor protein

C_c = critical concentration

CSF = cerebrospinal fluid

DTPA = diethylene triaminepentaacetic acid

PBS = phosphate-buffered saline

ROS = reactive oxygen species

SEC = size-exclusion chromatography

TEM = transmission electron microscopy

ThT = thioflavin T

XAS = X-ray absorption spectroscopy

REFERENCES

(1) Holtzman, D. M.; Morris, J. C.; Goate, A. M. *Sci. Transl. Med.* **2011**, *3*, 77sr1.

(2) Kuperstein, I.; Broersen, K.; Benilova, I.; Rozenski, J.; Jonckheere, W.; Debulpaep, M.; Vandersteen, A.; Segers-Nolten, I.; Van Der Werf, K.; Subramaniam, V.; Braeken, D.; Callewaert, G.; Bartic, C.; D'Hooge, R.; Martins, I. C.; Rousseau, F.; Schymkowitz, J.; De Strooper, B. *EMBO J.* **2010**, *29*, 3408−3420.

(3) Pauwels, K.; Williams, T. L.; Morris, K. L.; Jonckheere, W.; Vandersteen, A.; Kelly, G.; Schymkowitz, J.; Rousseau, F.; Pastore, A.; Serpell, L. C.; Broersen, K. *J. Biol. Chem.* **2012**, *287*, 5650−5660.

(4) Lovell, M. A.; Robertson, J. D.; Teesdale, W. J.; Campbell, J. L.; Markesbery, W. R. *J. Neurol. Sci.* **1998**, *158*, 47−52.

(5) Miller, L. M.; Wang, Q.; Telivala, T. P.; Smith, R. J.; Lanzirotti, A.; Miklossy, J. *J. Struct. Biol.* **2006**, *155*, 30−37.

(6) Opazo, C.; Huang, X.; Cherny, R. A.; Moir, R. D.; Roher, A. E.; White, A. R.; Cappai, R.; Masters, C. L.; Tanzi, R. E.; Inestrosa, N. C.; Bush, A. I. *J. Biol. Chem.* **2002**, *277*, 40302−40308.

(7) Reinke, A. A.; Gestwicki, J. E. *Chem. Biol. Drug Des.* **2011**, *77*, 399−411.

(8) Roychaudhuri, R.; Yang, M.; Hoshi, M. M.; Teplow, D. B. *J. Biol. Chem.* **2009**, *284*, 4749−4753.

(9) Viles, J. H. *Coord. Chem. Rev.* **2012**, *256*, 2271−2284.

(10) You, H.; Tsutsui, S.; Hameed, S.; Kannanayakal, T. J.; Chen, L.; Xia, P.; Engbers, J. D.; Lipton, S. A.; Stys, P. K.; Zamponi, G. W. *Proc. Natl. Acad. Sci. U.S.A.* **2012**, *109*, 1737−1742.

(11) Sparks, D. L.; Schreurs, B. G. *Proc. Natl. Acad. Sci. U.S.A.* **2003**, *100*, 11065−11069.

(12) Sanokawa-Akakura, R.; Cao, W.; Allan, K.; Patel, K.; Ganesh, A.; Heiman, G.; Burke, R.; Kemp, F. W.; Bogden, J. D.; Camakaris, J.; Birge, R. B.; Konsolaki, M. *PLoS One* **2010**, *5*, e8626.

(13) Chassaing, S.; Collin, F.; Dorlet, P.; Gout, J.; Hureau, C.; Faller, P. *Curr. Top. Med. Chem.* **2012**, *12*, 2573−2595.

(14) Smith, D. G.; Cappai, R.; Barnham, K. J. *Biochim. Biophys. Acta* **2007**, *1768*, 1976−1990.

(15) Frederickson, C. J. *Int. Rev. Neurobiol.* **1989**, *31*, 145−238.

(16) Hartter, D. E.; Barnea, A. *Synapse* **1988**, *2*, 412−415.

(17) Deshpande, A.; Mina, E.; Glabe, C.; Busciglio, J. *J. Neurosci.* **2006**, *26*, 6011−6018.

(18) Valensin, D.; Gabbiani, C.; Messori, L. *Coord. Chem. Rev.* **2012**, *19−20*, 2357−2366.

(19) Uversky, V. N.; Oldfield, C. J.; Dunker, A. K. *Annu. Rev. Biophys.* **2008**, *37*, 215−246.

(20) Hilbich, C.; Kisters-Woike, B.; Reed, J.; Masters, C. L.; Beyreuther, K. *J. Mol. Biol.* **1991**, *218*, 149−163.

(21) Barrow, C. J.; Zagorski, M. G. *Science* **1991**, *253*, 179−182.

(22) Vivekanandan, S.; Brender, J. R.; Lee, S. Y.; Ramamoorthy, A. *Biochem. Biophys. Res. Commun.* **2011**, *411*, 312−316.

(23) Danielsson, J.; Jarvet, J.; Damberg, P.; Graslund, A. *FEBS J.* **2005**, *272*, 3938−3949.

(24) Lazo, N. D.; Grant, M. A.; Condron, M. C.; Rigby, A. C.; Teplow, D. B. *Protein Sci.* **2005**, *14*, 1581−1596.

(25) Frieden, C. *Protein Sci.* **2007**, *16*, 2334−2344.

(26) Coles, M.; Bicknell, W.; Watson, A. A.; Fairlie, D. P.; Craik, D. J. *Biochemistry* **1998**, *37*, 11064−11077.

(27) Bertini, I.; Gonnelli, L.; Luchinat, C.; Mao, J.; Nesi, A. *J. Am. Chem. Soc.* **2011**, *133*, 16013−22.

(28) Paravastu, A. K.; Leapman, R. D.; Yau, W. M.; Tycko, R. *Proc. Natl. Acad. Sci. U.S.A.* **2008**, *105*, 18349−51834.

(29) Fandrich, M. *J. Mol. Biol.* **2012**, *421*, 427−440.

(30) Stroud, J. C.; Liu, C.; Teng, P. K.; Eisenberg, D. *Proc. Natl. Acad. Sci. U.S.A.* **2012**, *109*, 7717−7722.

(31) Alies, B.; Bijani, C.; Sayen, S.; Guillon, E.; Faller, P.; Hureau, C. *Inorg. Chem.* **2012**, *51*, 12988−13000.

(32) Hureau, C. *Coord. Chem. Rev.* **2012**, *256*, 2164−2174.

(33) Migliorini, C.; Porciatti, E.; Luczkowski, M.; Valensin, D. *Coord. Chem. Rev.* **2012**, *256*, 352−368.

(34) Tôugu, V.; Palumaa, P. *Coord. Chem. Rev.* **2012**, *256*, 2219−2224.

(35) Zawisza, I.; Rozga, M.; Bal, W. *Coord. Chem. Rev.* **2012**, *256*, 2297−2307.

(36) Hureau, C.; Dorlet, P. *Coord. Chem. Rev.* **2012**, *256*, 2175−2187.

(37) Dorlet, P.; Gambarelli, S.; Faller, P.; Hureau, C. *Angew. Chem., Int. Ed.* **2009**, *48*, 9273−9276.

(38) Kim, D.; Kim, N. H.; Kim, S. H. *Angew. Chem., Int. Ed.* **2013**, *52*, 1139−1142.

(39) Hureau, C.; Balland, V.; Coppel, Y.; Solari, P. L.; Fonda, E.; Faller, P. *J. Biol. Inorg. Chem.* **2009**, 995−1000.

(40) Damante, C. A.; Osz, K.; Nagy, N. V.; Pappalardo, G.; Grasso, G.; Impellizzeri, G.; Rizzarelli, E.; Sovago, I. *Inorg. Chem.* **2009**, *48*, 10405−10415.

(41) Faller, P.; Hureau, C. *Dalton Trans.* **2009**, 1080−1094.

(42) Bousejra-El-Garah, F.; Bijani, C.; Coppel, Y.; Faller, P.; Hureau, C. *Inorg. Chem.* **2011**, *50*, 9024−9030.
(43) Alies, B.; Renaglia, E.; Rozga, M.; Bal, W.; Faller, P.; Hureau, C. *Anal. Chem.* **2013**, DOI: 10.1021/ac302629u.
(44) Alies, B.; Badei, B.; Faller, P.; Hureau, C. *Chemistry* **2012**, *18*, 1161−1167.
(45) Faller, P. *ChemBioChem* **2009**, *10*, 2837−2845.
(46) Gunderson, W. A.; Hernandez-Guzman, J.; Karr, J. W.; Sun, L.; Szalai, V. A.; Warncke, K. *J. Am. Chem. Soc.* **2012**, *134*, 18330−18337.
(47) Karr, J. W.; Szalai, V. A. *Biochemistry* **2008**, *47*, 5006−5016.
(48) Sarell, C. J.; Syme, C. D.; Rigby, S. E.; Viles, J. H. *Biochemistry* **2009**, *48*, 4388−4402.
(49) Parthasarathy, S.; Long, F.; Miller, Y.; Xiao, Y.; McElheny, D.; Thurber, K.; Ma, B.; Nussinov, R.; Ishii, Y. *J. Am. Chem. Soc.* **2011**, *133*, 3390−3400.
(50) Mithu, V. S.; Sarkar, B.; Bhowmik, D.; Chandrakesan, M.; Maiti, S.; Madhu, P. K. *Biophys. J.* **2011**, *101*, 2825−2832.
(51) Miller, Y.; Ma, B. Y.; Nussinov, R. *Coord. Chem. Rev.* **2012**, *256*, 2245−2252.
(52) Giannozzi, P.; Jansen, K.; La Penna, G.; Minicozzi, V.; Morante, S.; Rossi, G.; Stellato, F. *Metallomics* **2012**, *4*, 156−165.
(53) Talmard, C.; Bouzan, A.; Faller, P. *Biochemistry* **2007**, *46*, 13658−13666.
(54) Jiang, D.; Zhang, L.; Grant, G. P.; Dudzik, C. G.; Chen, S.; Patel, S.; Hao, Y.; Millhauser, G. L.; Zhou, F. *Biochemistry* **2013**, *52*, 547−556.
(55) Shearer, J.; Callan, P. E.; Tran, T.; Szalai, V. A. *Chem. Commun.* **2010**, *46*, 9137−9139.
(56) Crescenzi, O.; Tomaselli, S.; Guerrini, R.; Salvadori, S.; D'Ursi, A. M.; Temussi, P. A.; Picone, D. *Eur. J. Biochem.* **2002**, *269*, 5642−5648.
(57) Lomakin, A.; Teplow, D. B.; Kirschner, D. A.; Benedek, G. B. *Proc. Natl. Acad. Sci. U.S.A.* **1997**, *94*, 7942−7947.
(58) Lee, C. F. *Phys. Rev. E* **2009**, *80*, 031922.
(59) Yoshimura, Y.; Lin, Y.; Yagi, H.; Lee, Y. H.; Kitayama, H.; Sakurai, K.; So, M.; Ogi, H.; Naiki, H.; Goto, Y. *Proc. Natl. Acad. Sci. U.S.A.* **2012**, *109*, 14446−14451.
(60) O'Nuallain, B.; Shivaprasad, S.; Kheterpal, I.; Wetzel, R. *Biochemistry* **2005**, *44*, 12709−12718.
(61) Stine, W. B., Jr.; Dahlgren, K. N.; Krafft, G. A.; LaDu, M. J. *J. Biol. Chem.* **2003**, *278*, 11612−11622.
(62) Ding, F.; Borreguero, J. M.; Buldyrey, S. V.; Stanley, H. E.; Dokholyan, N. V. *Proteins* **2003**, *53*, 220−228.
(63) Wetzel, R. *Trends Biotechnol.* **1994**, *12*, 193−198.
(64) Wetzel, R. *Acc. Chem. Res.* **2006**, *39*, 671−679.
(65) Bieschke, J.; Zhang, Q.; Bosco, D. A.; Lerner, R. A.; Powers, E. T.; Wentworth, P., Jr.; Kelly, J. W. *Acc. Chem. Res.* **2006**, *39*, 611−619.
(66) Schnabel, J. *Nature* **2011**, *475*, S12−S14.
(67) Bhak, G.; Choe, Y. J.; Paik, S. R. *BMB Rep.* **2009**, *42*, 541−551.
(68) LeVine, H., 3rd *Protein Sci.* **1993**, *2*, 404−410.
(69) Xue, W. F.; Homans, S. W.; Radford, S. E. *Proc. Natl. Acad. Sci. U.S.A.* **2008**, *105*, 8926−8931.
(70) Morris, A. M.; Watzky, M. A.; Finke, R. G. *Biochim. Biophys. Acta* **2009**, *1794*, 375−397.
(71) Atwood, C. S.; Perry, G.; Zeng, H.; Kato, Y.; Jones, W. D.; Ling, K.-Q.; Huang, X.; Moir, R. D.; Wang, D.; Sayre, L. M.; Smith, M. A.; Chen, S. G.; Bush, A. I. *Biochemistry* **2004**, *43*, 560−568.
(72) Leal, S. S.; Botelho, H. M.; Gomes, C. M. *Coord. Chem. Rev.* **2012**, *256*, 2253−2270.
(73) Bell, D. J.; Hoare, M.; Dunnill, P. *Adv. Biochem. Eng. Biotechnol.* **1983**, *26*, 1−72.
(74) Sengupta, P.; Garai, K.; Sahoo, B.; Shi, Y.; Callaway, D. J. E.; Maiti, S. *Biochemistry* **2003**, *42*, 10506−10513.
(75) Kodali, R.; Williams, A. D.; Chemuru, S.; Wetzel, R. *J. Mol. Biol.* **2010**, *401*, 503−517.
(76) Faller, P.; Hureau, C.; Dorlet, P.; Hellwig, P.; Coppel, Y.; Collin, F.; Alies, B. *Coord. Chem. Rev.* **2012**, *256*, 2381−2396.
(77) Tõugu, V.; Karafin, A.; Zovo, K.; Chung, R. S.; Howells, C.; West, A. K.; Palumaa, P. *J. Neurochem.* **2009**, *110*, 1785−1795.
(78) Pedersen, J. T.; Østergaard, J.; Rozlosnik, N.; Gammelgaard, B.; Heegaard, N. H. *J. Biol. Chem.* **2011**, *286*, 26952−26963.
(79) Burdick, D.; Soreghan, B.; Kwon, M.; Kosmoski, J.; Knauer, M.; Henschen, A.; Yates, J.; Cotman, C.; Glabe, C. *J. Biol. Chem.* **1992**, *267*, 546−554.
(80) Alies, B.; Eury, H.; Bijani, C.; Rechignat, L.; Faller, P.; Hureau, C. *Inorg. Chem.* **2011**, *50*, 11192−11201.
(81) Faller, P. *ChemBioChem* **2009**, *10*, 2837−2845.
(82) Pedersen, J. T.; Teilum, K.; Heegaard, N. H. H.; Østergaard, J.; Adolph, H.-W.; Hemmingsen, L. *Angew. Chem., Int. Ed.* **2011**, *50*, 2532−2535.
(83) Parthasarathy, S.; Long, F.; Miller, Y.; Xiao, Y.; McElheny, D.; Thurber, K.; Ma, B.; Nussinov, R.; Ishii, Y. *J. Am. Chem. Soc.* **2011**, *133*, 3390−3400.
(84) Karr, J. W.; Kaupp, L. J.; Szalai, V. A. *J. Am. Chem. Soc.* **2004**, *126*, 13534−13538.
(85) Talmard, C.; Guilloreau, L.; Coppel, Y.; Mazarguil, H.; Faller, P. *ChemBioChem* **2007**, *8*, 163−165.
(86) Lim, K. H.; Kim, Y. K.; Chang, Y.-T. *Biochemistry* **2007**, *46*, 13523−13532.
(87) Mekmouche, Y.; Coppel, Y.; Hochgrafe, K.; Guilloreau, L.; Talmard, C.; Mazarguil, H.; Faller, P. *ChemBioChem* **2005**, *6*, 1663−1671.
(88) Rezaei-Ghaleh, N.; Giller, K.; Becker, S.; Zweckstetter, M. *Biophys. J.* **2011**, *101*, 1202−1211.
(89) Kirkitadze, M. D.; Condron, M. M.; Teplow, D. B. *J. Mol. Biol.* **2001**, *312*, 1103−1119.
(90) Chen, Y. R.; Huang, H. B.; Chyan, C. L.; Shiao, M. S.; Lin, T. H.; Chen, Y. C. *J. Biochem.* **2006**, *139*, 733−740.
(91) Talmard, C.; Leuma Yona, R.; Faller, P. *J. Biol. Inorg. Chem.* **2009**, *14*, 449−455.
(92) Solomonov, I.; Korkotian, E.; Born, B.; Feldman, Y.; Bitler, A.; Rahimi, F.; Li, H.; Bitan, G.; Sagi, I. *J. Biol. Chem.* **2012**, *287*, 20555−20564.
(93) Smith, D. P.; Ciccotosto, G. D.; Tew, D. J.; Fodero-Tavoletti, M. T.; Johanssen, T.; Masters, C. L.; Barnham, K. J.; Cappai, R. *Biochemistry* **2007**, *46*, 2881−2891.
(94) Garai, K.; Sengupta, P.; Sahoo, B.; Maiti, S. *Biochem. Biophys. Res. Commun.* **2006**, *345*, 210−215.
(95) Chen, W. T.; Liao, Y. H.; Yu, H. M.; Cheng, I. H.; Chen, Y. R. *J. Biol. Chem.* **2011**, *286*, 9646−9656.
(96) Innocenti, M.; Salvietti, E.; Guidotti, M.; Casini, A.; Bellandi, S.; Foresti, M. L.; Gabbiani, C.; Pozzi, A.; Zatta, P.; Messori, L. *J. Alzheimers Dis.* **2010**, *19*, 1323−1329.
(97) Ha, C.; Ryu, J.; Park, C. B. *Biochemistry* **2007**, *46*, 6118−3125.
(98) Sarell, C. J.; Wilkinson, S. R.; Viles, J. H. *J. Biol. Chem.* **2010**, *285*, 41533−41540.
(99) Mantyh, P. W.; Ghilardi, J. R.; Rogers, S.; DeMaster, E.; Allen, C. J.; Stimson, E. R.; Maggio, J. E. *J. Neurochem.* **1993**, *61*, 1171−1174.
(100) Klug, G. M.; Losic, D.; Subasinghe, S. S.; Aguilar, M. I.; Martin, L. L.; Small, D. H. *Eur. J. Biochem.* **2003**, *270*, 4282−4293.
(101) Esler, W. P.; Stimson, E. R.; Jennings, J. M.; Ghilardi, J. R.; Mantyh, P. W.; Maggio, J. E. *J. Neurochem.* **1996**, *66*, 723−732.
(102) Brown, A. M.; Tummolo, D. M.; Rhodes, K. J.; Hofmann, J. R.; Jacobsen, J. S.; Sonnenberg-Reines, J. *J. Neurochem.* **1997**, *69*, 1204−1212.
(103) Suzuki, K.; Miura, T.; Takeuchi, H. *Biochem. Biophys. Res. Commun.* **2001**, *285*, 991−996.
(104) Bush, A. I.; Pettingell, W. H.; Multhaup, G.; Paradis, M.; Vonsattel, J. P.; Gusella, J. F.; Beyreuther, K.; Masters, C. L.; Tanzi, R. E. *Science* **1994**, *265*, 1464−1467.
(105) House, E.; Mold, M.; Collingwood, J.; Baldwin, A.; Goodwin, S.; Exley, C. *J. Alzheimers Dis.* **2009**, *18*, 811−7.
(106) Yoshiike, Y.; Tanemura, K.; Murayama, O.; Akagi, T.; Murayama, M.; Sato, S.; Sun, X.; Tanaka, N.; Takashima, A. *J. Biol. Chem.* **2001**, *276*, 32293−32299.
(107) Noy, D.; Solomonov, I.; Sinkevich, O.; Arad, T.; Kjaer, K.; Sagi, I. *J. Am. Chem. Soc.* **2008**, *130*, 1376−1383.

(108) Zou, J.; Kajita, K.; Sugimoto, N. *Angew. Chem., Int. Ed.* **2001**, *40*, 2274−2277.
(109) House, E.; Collingwood, J.; Khan, A.; Korchazkina, O.; Berthon, G.; Exley, C. *J. Alzheimers Dis.* **2004**, *6*, 291−301.
(110) Huang, X.; Atwood, C. S.; Moir, R. D.; Hartshorn, M. A.; Tanzi, R. E.; Bush, A. I. *J. Biol. Inorg. Chem.* **2004**, *9*, 954−960.
(111) Bica, L.; Crouch, P. J.; Cappai, R.; White, A. R. *Mol. Biosyst.* **2009**, *5*, 134−142.
(112) Roberts, B. R.; Ryan, T. M.; Bush, A. I.; Masters, C. L.; Duce, J. A. *J. Neurochem.* **2012**, *120*, 149−166.
(113) Pithadia, A. S.; Lim, M. H. *Curr. Opin. Chem. Biol.* **2012**, *16*, 67−73.
(114) Rodriguez-Rodriguez, C.; Telpoukhovskaia, M.; Orvig, C. *Coord. Chem. Rev.* **2012**, *256*, 2308−2332.
(115) Barnham, K. J.; Kenche, V. B.; Ciccotosto, G. D.; Smith, D. P.; Tew, D. J.; Liu, X.; Perez, K.; Cranston, G. A.; Johanssen, T. J.; Volitakis, I.; Bush, A. I.; Masters, C. L.; White, A. R.; Smith, J. P.; Cherny, R. A.; Cappai, R. *Proc. Natl. Acad. Sci. U.S.A.* **2008**, *105*, 6813−6818.
(116) Kumar, A.; Moody, L.; Olaivar, J. F.; Lewis, N. A.; Khade, R. L.; Holder, A. A.; Zhang, Y.; Rangachari, V. *ACS Chem. Neurosci.* **2010**, 691−701.
(117) Ma, G.; Huang, F.; Pu, X.; Jia, L.; Jiang, T.; Li, L.; Liu, Y. *Chemistry* **2011**, *17*, 11657−11666.
(118) Sasaki, I.; Bijani, C.; Ladeira, S.; Bourdon, V.; Faller, P.; Hureau, C. *Dalton Trans.* **2012**, *41*, 6404−6407.
(119) Collin, F.; Sasaki, I.; Eury, H.; Faller, P.; Hureau, C. *Chem. Commun.* **2013**, *49*, 2130−2132.
(120) Valensin, D.; Anzini, P.; Gaggelli, E.; Gaggelli, N.; Tamasi, G.; Cini, R.; Gabbiani, C.; Michelucci, E.; Messori, L.; Kozlowski, H.; Valensin, G. *Inorg. Chem.* **2010**, *49*, 4720−4722.